Damascus University Journal of Earthquake and Disaster Research
مجلة جامعة دمشق لبحوث الزلازل والكوارث
Vo 3 number (1) -2026: 37-50
المجلد 3 العدد (1) – 2026: 37-50

Inelastic Attenuation of Body Waves in Southern Syria

Mohamad Yasser sharaf aldein*[1] Khaled omar[2] Mohamad khair abdul-wahed[3]

*[1]. Master`s degree Student, Department of Seismology, Higher Institute of Earthquake studies &Research, Damascus University.
Yaser.sharaf@damascusuniversity.edu.sy

[2]. Professor Assistant, Department of Seismology, Higher Institute of Earthquake studies &Research, Damascus University.
Khald.omar@damascusuniversity.edu.sy

[3]. Doctor, researcher at Atomic energy commission.
mabdulwahed@aec.org.sy

Received: 19/12/2025
Accepted: 6/4/2026

Abstract:

This study provides a detailed explanation of inelastic attenuation, first within its theoretical framework, including an explanation of the effect of wave paths through the depths of the earth's crust from the source toward the receiver within heterogeneous and tectonically active media, and the reflection of this path on the waves through attenuation, which appears as intrinsic (transformational) attenuation and scattering attenuation. This is followed by an explanation of the mathematical relationships of attenuation and coda waves, along with an overview of the attenuation calculation methods used by researchers in previous studies and reference research. Second, the practical framework includes the steps followed to calculate attenuation using the Coda Wave Decay Method, which was applied to the southern Syria region using 31 seismic events recorded at the National Earthquake Center on 38 stations, with a total of (210) seismic recordings between (2009-2024), with magnitudes ranging between (2-5), at central frequencies (1-24) Hz, for a total of 7 central frequencies. The attenuation calculations resulted in contour maps representing the variations of the quality factor for each central frequency separately, in addition to extracting the basic attenuation parameters (Q0, α), and subsequently obtaining the general attenuation equation for the study area, which takes the form :

$\boldsymbol{Qc = 130 \mp 26 \,.\, f^{0.81\mp0.}}$, where the relatively low Q0 values (130) indicate

that attenuation is high in the studied area due to the spread of tectonic deformations and faults, and the high values of the constant (α) (0.81) indicate a strong dependence of attenuation on frequency in the studied area.

Keywords: Quality factor, inelastic attenuation, coda waves, coda wave decay method.

التخامد اللامرن للأمواج الجسمية في جنوب سورية

محمد ياسر شرف الدين*[1] خالد عمر[2] محمد خير عبد الواحد[3]

[1*] طالب ماجستير، قسم علم الزلازل، المعهد العالي للبحوث والدراسات الزلزالية، جامعة دمشق.
Yaser.sharaf@damascusuniversity.edu.sy

[2] مدرس، قسم علم الزلازل، المعهد العالي للبحوث والدراسات الزلزالية.
Khald.omar@damascusuniversity.edu.sy

[3]. دكتور، باحث في هيئة الطاقة الذرية.
mabdulwahed@aec.org.sy

الملخص:

تم في هذا البحث شرح مفصل للتخامد اللامرن بإطاره النظري أولاً، متضمناً شرح تأثير مسير الأمواج ضمن أعماق القشرة الأرضية من المنبع باتجاه المستقبِل ضمن أوساط غير متجانسة ونشطة تكتونياً، وانعكاس هذا المسير على الأمواج من خلال التخامد الذي يظهر بشكل تخامد تحولي وتخامد تبعثري، ومن ثم شرح العلاقات الرياضية للتخامد، وأمواج كودا مع لمحة عن طرائق حساب التخامد كما ساقه الباحثون فيما سبق من الدراسات والأبحاث المرجعية. والإطار العملي ثانياً، ويتضمن الخطوات المتبعة لحساب التخامد بطريقة تلاشي أمواج كودا (Coda wave Decay Method) بحيث طبقت هذه الطريقة على منطقة جنوب سورية باستخدام 31 حدث زلزالي مسجل في المركز الوطني للزلازل في 38 محطة بمجموع (210) تسجيل زلزالي بين عامي (2009–2024) بقدور تتراوح بين (2–5) على ترددات مركزية (1–24) هرتز بمجموع 7 ترددات مركزية. نتج عن حسابات التخامد خرائط كونتورية ممثلة لتغيرات معامل الجودة مقابل كل تردد مركزي على حدة، إضافة لاستخراج معاملات التخامد الأساسية (Q0، α) ومن ثم الحصول على المعادلة العامة للتخامد في منطقة الدراسة لتكون بالشكل $Qc = 130 \mp 26 \,.\, f^{0.81 \mp 0.08}$ بحيث أظهرت قيم Q0 المنخفضة نسبياً (130) كون التخامد عالي في المنطقة المدروسة بسبب انتشار التشوهات التكتونية و الصدوع ، وقيم الثابت (α) المرتفعة (0.81) الارتباط العالي للتخامد بالتردد في المنطقة المدروسة.

الكلمات المفتاحية: معامل الجودة، التخامد اللامرن، أمواج كودا، طريقة تلاشي أمواج كودا.

تاريخ الايداع: 2025/12/19
تاريخ القبول: 2026/4/6

Introduction:

Seismic waves are affected, during the path they travel, by the properties of the rocks within the earth's crust and by the interfaces between geological layers, causing a decrease in their amplitude known as attenuation. Attenuation falls within the path effect, which affects the waveform of the seismic signal in addition to the effect of the source and the site. Physically, the attenuation of seismic waves is defined as: the decrease in the amplitude of seismic waves as they propagate through the layers of the earth's crust, resulting from geometrical spreading and scattering attenuation due to the heterogeneity of the medium's properties, in addition to intrinsic absorption resulting from the friction of the rock grains that make up the earth's crust (Padhy et al. 2011) [1]. The study of the layer quality factor (Q) plays an important role in studies of the structure of the earth's crust, as useful information about the properties of the medium can be inferred, which is necessary for seismic hazard studies and assessment. Over the past three decades, various studies have been used in many parts of the world (Azzaro et al., 2013; Del Pezzo et al., 2016; Singh et al., 2016; Giampiccolo, 2018), where the study of the layer quality factor (Q) relies on coda waves from small earthquakes to determine the attenuation characteristics of the crust. The wide variety of paths through which these scattered waves travel provides a range of information related to the properties of the medium, and the attenuation of seismic waves in the lithosphere depends heavily on frequency, resulting from a combination of two effects: scattering and inelastic attenuation, which are difficult to separate from one another, since each has a similar dependence on travel time or distance. Inelastic attenuation depends heavily on the tectonic environment, as shown in numerous studies conducted in different parts of the world (for example, Havskov et al. 1989) [2].

1- References Review:

(محمد، 2012) studied the propagation characteristics of local and regional seismic waves in Syria, which allowed for characterizing the propagation properties and behavior of the various wave phases for more than 340 earthquakes recorded at 57 seismic monitoring stations in the Syrian national network or neighboring networks in Turkey, Cyprus, and Jordan. This was done by applying the Seismic Tomography Technique, in which the Lg wave phase, which carries most of the energy released by large earthquakes to distances exceeding 150 km, was studied. A two-dimensional tomographic model was developed for the variations of ηLg and LgQ0 values for Syria and neighboring regions. The calculated Q0 values ranged between (60 and 400). It was also indicated that LgQ0 values ranged between 150–225 in the southwestern region, which is low compared to other regions, due to variations in the thickness of the earth's crust and plate deformation processes that lead to a rise in temperature, in addition to the wide distribution of volcanic deposits. In the southern region, however, the Q0 value reaches 300 within the Al-Rutba uplift zone and eastern Jordan [3].

(قنواتي، 2024) carried out magnitude calculations for about 449 tremors, with relocation of the tremors' epicenters using one, two, and three stations. The locations of tremors shared with the Lebanese and Syrian networks were also relocated by combining the readings of the Lebanese and Syrian monitoring stations with the stations used in the research, which gave more accurate results due to the increased number of monitoring station readings. The crustal wave phases and their different paths from the seismic focus to the recording stations were then studied, and travel times, amplification, and the quality factor (Q) were calculated using the coda wave method to determine the propagation characteristics of microseismic waves in the geological structures of the study area. The quality factor results showed that the Qalamoun region is characterized by high attenuation resulting from its complex tectonic structure, such that the attenuation value calculations in the region produced attenuation contour maps at central frequencies (16, 8, 4, 2) [4].

Later, (Bao et al., 2011) produced a seismic attenuation map of the regional Pg phase for the northern Middle East region using frequency-dependent Q measurements from two stations and seismic attenuation tomography. The attenuation cross-sectional images in the northeastern Mediterranean show large variations in the (Qpg) value, which may be due to variations in the crustal composition itself; a large diversity is also observed in the (Qpg) pattern, such as low (Qpg) values within the Anatolian plate and high (Qpg) values within most of the Arabian plate [5].

(Sandvol et al., 2001) then used a large dataset of local and regional recordings registered in the Middle East, amounting to about 5000 seismic recordings from 65 stations and 2200 events, aiming to analyze the characteristics and propagation pattern of regional seismic waves. A map of efficient and inefficient propagation zones for (Lg), (Pg), and (Sn) across the Middle East was also produced, using two tomographic techniques developed to identify lithospheric attenuation zones within the Middle East. The results showed evidence of large increases in Lg attenuation, relative to Pg, in the Bitlis suture zone, the Zagros folds, and the thrust belts at the boundary between the Arabian and Eurasian plates. Zones of inefficient Sn propagation were also observed along the Dead Sea Fault System (DSFS) [6].

2-Tectonic and Geological Description:

With respect to the main structural units in Syria, the study area is part of the relatively stable zone of the Arabian plate margin, characterized by a shallow basement and the absence of differentiation within the thin, gently folded sedimentary cover (حسين، 2012). This includes each of the following [7]:

A- Jordan Uplift:

It appears in Syria at its northern end. Its cross-section forms a massive arch, with a steeply dipping western limb and a gently dipping eastern limb. It is bounded on the west by the strike-slip (rift) valley of the Jordan River, which belongs to the northern segment of the Grand African Fault System and is considered a continuation of it. The rift valley is filled with a large thickness of Neogene and Quaternary sediments, mainly of lacustrine origin. The rocks of the uplift itself belong to the Triassic–Jurassic–Cretaceous. Recent tectonic movements have raised the Pliocene sediments, under the influence of faulting, to a level higher than the floor of the rift valley [7].

B- Jabal Al-Arab Depression:

This depression is filled with a large thickness of horizontally deposited Neogene and Quaternary basaltic flows. It is likely that the underlying Paleogene and pre-Paleogene sediments in this region are of greater thickness than those on the slopes of the Al-Rutba and Jordan uplifts.

The structure of the Jabal Al-Arab depression is complicated by a set of faults trending northwest, parallel to the axis of this depression, and these faults are marked by rows of volcanic peaks following the same direction. These faults are deep, since they were used over a long period of their development as conduits for the discharge of lava flows. The extensive volcanic activity in this depression is linked to the development of the Levant strike-slip system [7].

C- Al-Rutba Uplift:

The core of this uplift (arch) consists of Triassic and Jurassic rocks whose layers are deposited nearly horizontally, or with a slight dip. The northern slope of the uplift, on the other hand, consists of Cretaceous and Paleogene sediments showing gentle folds of the Brachy Anticline type, the largest of which have an oval shape (in cross-section). Their axes range in length from 10–80 km and in width from 5.5 km. The arches (upper part or crest) of these folds consist of horizontally deposited Lower Eocene rock layers. The dip of the limbs of these longitudinal anticlines is estimated at (1–2)° and rarely reaches (3–5)°. The arches of the large anticlines are clearly visible at the surface as uplifted landforms, while local depressions occur between a number of these longitudinal anticlines. These depressions are filled with Neogene and Quaternary sediments, Figure (1).

The Al-Rutba uplift is bounded on the north by a set of transverse faults whose traces appear on the terrain as longitudinal ridges. Along their extent, breccia-type rocky zones are observed to be widespread. The fault planes of some of these faults are visible, and folded rock layers are also found adjacent to them, in addition to some volcanic cones. The transverse faults extend for 150–200 km, yet they have a relatively small throw (a few tens of meters). These faults are accompanied by a large number of fractures distributed either parallel to the fault direction or perpendicular to it.

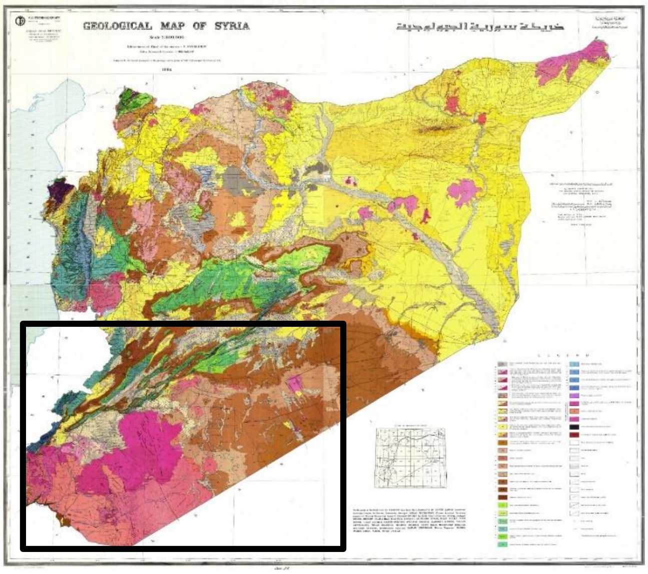

Figure (1) Geological map of Syria; the box represents the studied area. The map is from the official website of the (Geological Institute, Russian Academy of Sciences)

4-Method:

Coda waves form the tail end of the seismic signal for local and regional events, beginning to arrive after the shear wave (S). Coda waves consist of incoherent waves scattered due to heterogeneity, and their amplitude is believed to decrease only due to attenuation (including scattering) and geometrical spreading. The decay of the coda amplitude A(f, t) as a function of frequency f and time t can be expressed as follows [8]:

$$A(f,t) = t^{-\beta} A_0 e^{\frac{-\pi f t}{Q_c(f)}}, \qquad \textbf{(1)}$$

where A0 is the initial amplitude, β is the geometrical spreading coefficient (1.0 for body waves, 0.75 for diffracted waves, and 0.5 for surface waves), and Qc is the coda attenuation.

The geometrical spreading coefficient is usually assumed to equal 1.0, given the use of the early part of the wave peak for local earthquakes. By taking logarithms and rearranging, equation (1) can be written as follows [8]:

$$\ln[A(f,t)] + \beta \ln(t) = \ln(A_0) - \frac{t f \pi}{Q_c(f)}. \qquad \textbf{(2)}$$

Plotting the curve (the first term of equation (2)) as a function of t, at a given central frequency (by filtering the signal around the central frequency within the passband), gives a straight line with a slope of (−πf/Qc(f)), and Qc(f) can be determined using least squares.

The curve can be obtained by computing the root-mean-square (rms) values within a running window of specified length, starting at a specified time, the elapsed time, and after the event onset time. Alternatively, the curve is sometimes computed using the envelope definition together with the Hilbert transform H, as follows [8]:

$$\text{Envelope}(f,t) = \sqrt{H[A(f,t)]^2 + A(f,t)^2}. \quad)3($$

This method is called the coda wave decay method [8] (CWD: Coda Wave Decay Method), and it is the most widely used method for determining coda Q. It has been applied in numerous scientific studies, such as (Bianco et al., 2002; Mak et al., 2004; Mukhopadhyay et al., 2008; Carcole and Sato, 2010; Calvet and Margerin, 2013; Singh et al., 2015).

(Kumar et al., 2006) noted that the determination of Qc is not affected by near-surface attenuation, nor by soil amplification [9].

Coda Q (Qc) is believed to consist of scattering Q and intrinsic Q. Recent studies have been more consistent in finding that Qsc dominates at short distances (0–100 km), while Qi dominates at greater distances; for example, at a lapse time of 80 seconds, close agreement was found between Qi and Qc [8].

It was also observed that there is a frequency-dependent difference for data at short distances. At frequencies below 6 Hz, scattering was dominant, whereas intrinsic attenuation was dominant at frequencies above 6 Hz [8].

$$Q_c = Q_0(f/f_0)^{\alpha}, \quad \textbf{(4)}$$

where Q0 is the value of Q at a reference frequency f0, and α is a constant. Most studies assume f0 = 1 Hz, so that the equation then takes the form [8]:

$$Q_c = Q_0 f^{\alpha}, \quad \textbf{(5)}$$

Equation (5) is the general attenuation equation.

The Seisan program is used to calculate attenuation by adding the seismic event recordings to the program, then identifying the main wave arrivals, in addition to determining the elapsed time by entering the attenuation calculation parameters into the Seisan program (Havskov, 2016), such that it is twice the S-wave arrival time [8], followed by applying filtering using a Butterworth filter at 7 central frequencies (1-2-4-8-10-16-24).

The quality factor values for the central frequencies are obtained and assigned to the midpoint between the source and the station. The resulting values are used to draw contour maps representing the quality factor isolines within the study area. From these values, the Q0 and α values can be obtained, and by substituting them into the general attenuation equation, the attenuation equation for the study area is derived.

5-Data:

The method described above was applied to 31 seismic events recorded at 38 monitoring stations, providing a total of 210 seismic recordings suitable for applying the research methodology. Table (1) presents some details about these seismic events, and Figure (2) then shows the map of the epicenters of these events.

Table (1) Information on the events studied in this research, including epicenter location, time, and magnitude

No.	year	month	date	hr	min	sec	Longitud	Latitude	depth	Ml
1	2009	12	20	0	25	23.8	35.339	33.207	0	2.4
2	2010	3	20	18	45	29.6	35.676	32.931	0	3.1
3	.2010	3	27	0	5		35.697	33.66	6.3	2
4	2010	11	14	18	48	13.4	35.551	33.097	0.9	2.5
5	2011	1	1	16	31		35.677	32.712	10	3.4
6	2011	1	20	21	38	49.7	35.51	33.052	0	3.2
7	2011	6	8	21	26		35.793	33.264	10	2
8	2011	9	21	21	56	6	35.375	33.329	5.8	2.7
9	2012	4	21	6	17	15.1	39.522	33.965	38.3	3.1
10	2012	4	22	8	17	46.2	37.449	34.65	235.2	3
11	2012	7	3	10	54	19.2	40.589	33.377	341.2	3
12	2012	7	10	17	35	2.8	35.579	33.072	4.2	2.9
13	2012	11	18	3	54	4.6	35.455	33.083	15.2	2.9
14	2012	12	3	5	14	49.9	34.65	33.672	13.5	3.1
15	2013	5	1	6	50	53	41.075	34.331	16.7	3.6
16	2013	10	17	18	17	53.2	35.612	32.812	8.5	3.1
17	2013	10	20	12	54	6.4	35.622	32.82	6.8	3.2
18	2018	4	17	15	45	33.1	36.959	33.923	31.9	3.3
19	2018	7	8	21	42	47.7	35.755	32.812	2.4	3
20	2018	7	22	6	41	28	35.791	32.801	3.8	3.4
21	2018	7	27	8	51	20.7	35.756	32.869	14.9	3.2
22	2018	11	3	17	42	52.8	35.195	33.712	34.4	3.3
23	2020	2	6	4	53	58.2	35.377	32.752	101	4.2
24	2020	4	22	13	55	35.8	38.461	33.323	104.8	3
25	2020	6	5	5	23	2.2	35.401	33.075	0	2.5
26	2022	5	15	20	14	21.5	35.784	33.884	0	2.2
27	2022	9	21	18	22	56.7	35.955	33.905	0.9	2.2
28	2022	11	18	11	36	22.6	35.326	33.434	0	2.8
29	2023	6	3	11	15	43	35.874	33.887	10	2.5
30	2024	3	12	3	59	51.6	35.806	33.418	9.7	2.4
31	2024	3	13	10	50	31.8	35.632	32.95	18	3.7

Figure (2) Distribution of the recorded events used in the attenuation calculation

6-Results and Discussion:

The attenuation calculations using the Seisan program [10] produced quality factor values for each central frequency separately, and these values were entered into the Surfer program in order to obtain contour maps of the quality factor isolines, representing the variations of the quality factor within the study area.

- The General Attenuation Equation:

After plotting the isoline maps of the quality factor variations in the study area, the average values of Q0 and α can be obtained from the Seisan program calculations, which are (130, 0.81), respectively.

By substituting into the general form of the attenuation equation, the attenuation equation for the study area is as follows, Equation (6):

$$Qc = 130 \mp 26 \, . \, f^{0.81 \mp 0.08} \qquad (6)$$

The parameters and equations specific to a group of stations within the region can also be shown in Table (2):

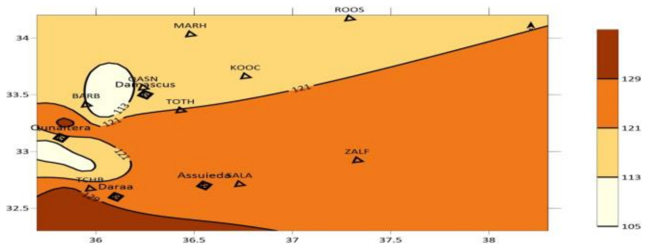

Q0

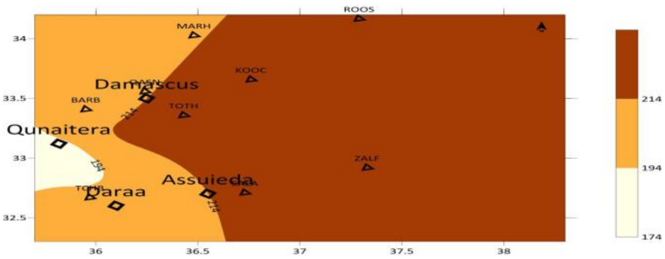

Q2

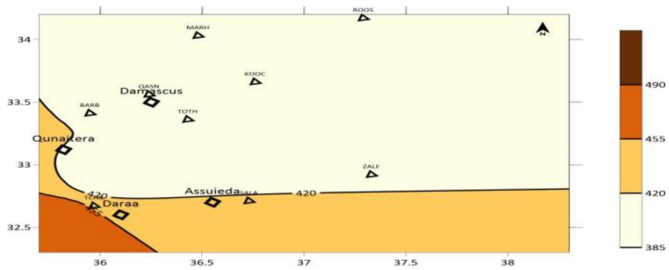

Q4

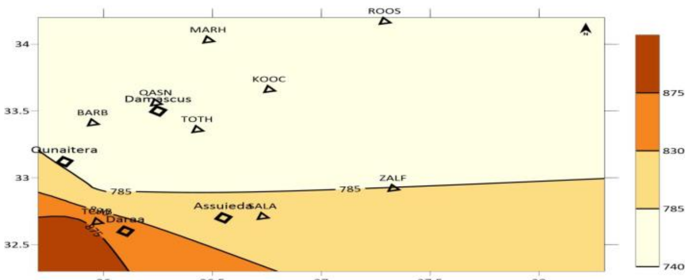

Q8

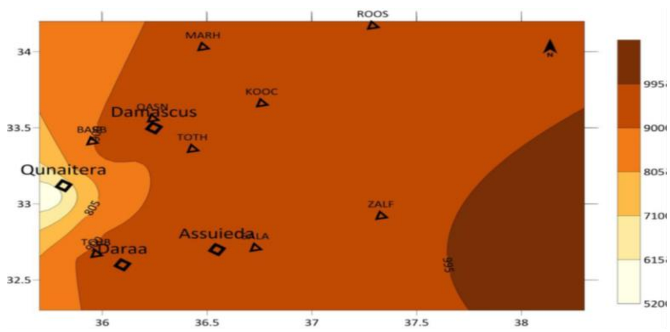

Q10

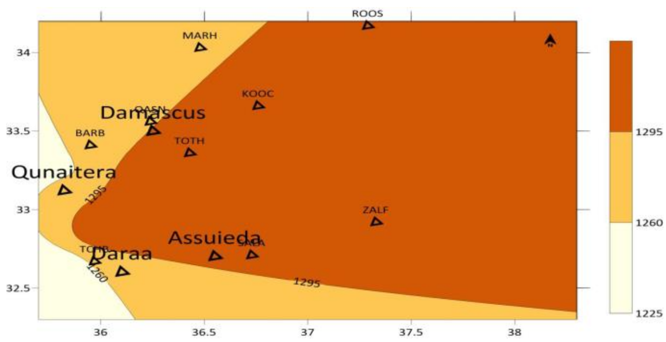

Q16

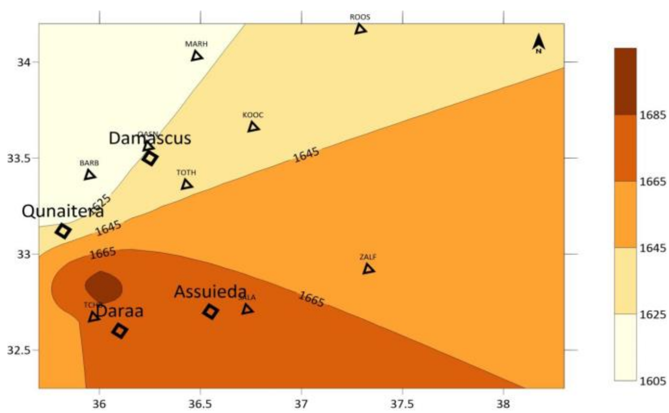

Q24

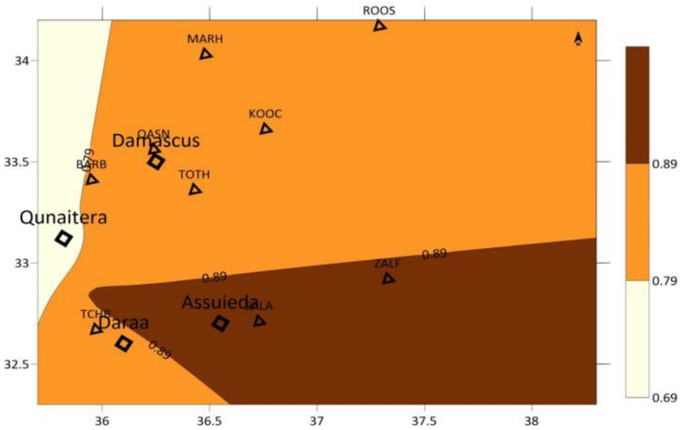

α

Figure (3) Quality factor contour maps at central frequencies (from 1–24), in addition to the α variation map

Table (2) Attenuation equation values at five of the stations that recorded the studied events

Station name	Attenuation equation
BARB	$Qc = 135 \mp 19 .f^{0.77\mp 0.05}$
TCHB	$Qc = 122 \mp 13 .f^{0.85\mp 0.04}$
TOTH	$Qc = 107 \mp 8 .f^{0.87\mp 0.04}$
QASN	$Qc = 125 \mp 38 .f^{0.93\mp 0.13}$
QNTR	$Qc = 114 \mp 23 .f^{0.93\mp 0.11}$

Low Q0 values indicate areas of low quality, dominated by high tectonic deformation and significant lithological heterogeneity, and consequently high attenuation values, and vice versa.

(محمد، 2012) observed that LgQ0 values ranged between 150–225 in the southwestern region, which is low compared to other regions, due to variations in the thickness of the earth's crust and plate deformation processes that lead to a rise in temperature, in addition to the wide distribution of volcanic deposits. In the southern region, however, the Q0 value reaches 300 within the Al-Rutba uplift zone and eastern Jordan [3].

The relatively low Q0 in the lower frequency ranges is attributed to energy loss due to the presence of numerous heterogeneities and reduced rock strength. Comparing the Q0 values from this research with previous studies, the Q0 values are low, indicating high wave attenuation, particularly in the southwestern region, which is an area of high tectonic deformation, especially due to its proximity to the Dead Sea Fault systems and the spread of volcanic rocks (with Q0 values reaching up to 100). The quality factor value increases toward the south (reaching up to 130) and the southeast, since the southern region is more stable.

The areas represented on the map with the lowest quality factor value (in white) are the areas of high tectonic deformation; the first represents the Qasioun Mountain area (in the shape of a circular sector), and the second represents the area closest to the Dead Sea Fault.

These two areas are characterized by being mountainous regions full of faults, which explains the low quality factor values, and consequently wave attenuation is at its highest compared to the rest of the study area.

High α values indicate a greater dependence of attenuation on frequency (given that the α value across the study area is above 0.5). (Giampiccolo, 2018) showed that this result falls within the expected values for areas of high lithological variability, high tectonic complexity, and high seismic activity [11]. A relatively low α value is observed within the study area in the region surrounding Quneitra toward the east (with an average of 0.81). Table (3) presents a comparison between the Q0 and α values of this study and a group of studies from around the world:

Table (3) shows large differences in the attenuation parameter values (Q0 and α) among attenuation studies worldwide, and these values vary depending on the study areas, their tectonic characteristics, and the level of heterogeneity prevailing in each region.

In the study by (Del Pezzo et al. (2015)), Q0 values as low as (30) appear, while α reached up to (0.5) [12].

The author attributes this to the fact that the study area (the Etna volcano region) is a volcanic area characterized by diverse heterogeneities, including faults in different directions and magmatic intrusions within the crust, as well as sources of heat flow and others, which play an important role in raising attenuation values in the region and consequently lowering the quality factor values.

In (Parvez et al. (2008)), the attenuation parameter values (Q0 and α) in the study area were (119, 0.9), respectively, and the author attributed this to the region having high tectonic activity, which also causes high attenuation [13].

On the other hand, the attenuation parameter values (Q0 and α) in (Pulli (1984)) were (460, 0.4), indicating low attenuation values, since the study area has stable tectonic activity [14].

Table (3) Comparative study of Q0 and α values with a group of results from studies around the world; the table is from (Giampiccolo, 2018)

Region	Q0	α	Source
Southern Syria	130	0.81	This study
Mts. Peloritani (northeastern Sicily)	50	0.7	Giampiccolo(.2018)
Messina Strait (southern Italy)	76	0.5	Tuvè et al. (2006)
Southern Spain	86	0.8	Ibanez et al. (1990)
Almeria Basin (Iberian Peninsula)	63	0.9	Pujades et al. (1990)
Taiwan	93	0.8	Chung et al. (2009)
Pannonian Basin (Croazia)	120	0.7	Dasovic et al. (2013)
Eastern Himalaya	111	1.1	Singh et al. (2016)
Andaman Islands	119	0.9	Parvez et al. (2008)
Abu Dabbab (Egypt)	20	0.9	Abdel-Fattah et al.2008)
Washington State (USA)	63	0.9	Havskov et al. (1989)
Koyna (India)	96	1.1	Gupta et al. (1998)
Mt. Etna (Italy)	30	0.5	Del Pezzo et al. (2015)
Volcan de Colima (Mexico)	92	0.5	Domínguez et al. (2003)
Norway	120	1.1	Kvamme and Haskov (1989)
New England	460	0.4	Pulli (1984)
Northeastern Brazil	151	0.9	Dias and Souza (2004)

In another comparison between the Q0 and α values and one of the previous studies, Figure (4):

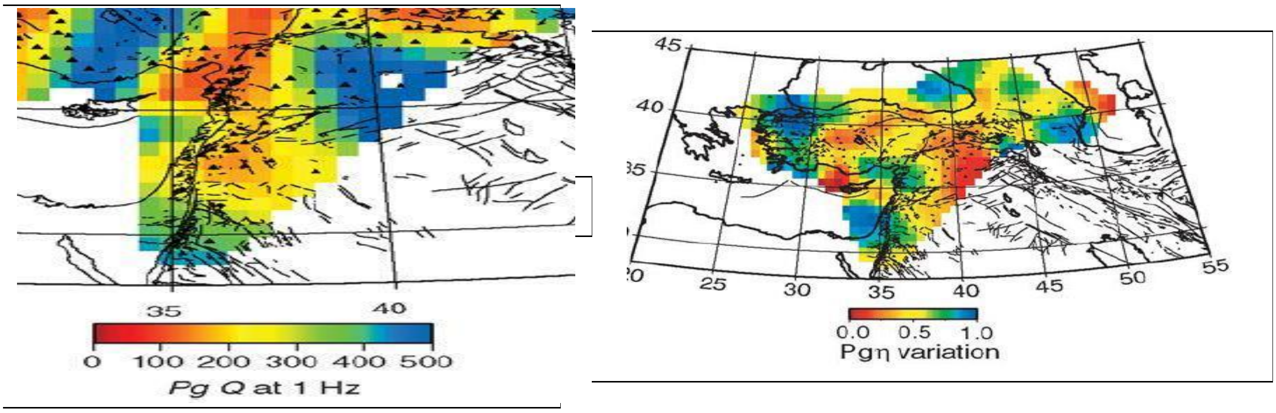

Figure (4) Variations of the PgQ and PGn values in Syria; the figure is from (Bao et al., 2011)

The Q0 value variations from (Bao et al., 2011) show that the color scale reflects a diversity of values, ranging between (100–300) in southern Syria and reaching up to (400) in northern Jordan [5]. These variations continue toward the north, reaching values of up to (300–500) in the northeastern part of Syria. Since the median Q0 value in this research was 130 (as in Equation (6)), the obtained values are similar to the Q0 values from (Bao et al., 2011). As for α, it ranges between (0–0.5) in the northeast and increases toward the northwest to reach 1. In the south, its value is between (0.5–1), which is close to the average value of the α factor in this research (0.81).

7-Conclusions:

Accordingly, the following results emerge from the above:

1- The basic attenuation parameters (Q0 and α) were extracted from a number of seismic recordings totaling 31 seismic events in southern Syria, recorded at 38 stations with a total of 210 seismic recordings, and the values of these parameters were (Q0 = 130) and (α = 0.81). Thus, the attenuation equation for the study area was obtained:

$$Qc = (130 \mp 26).\ f^{0.81 \mp 0.08}$$

2- As a result of plotting contour maps of the quality factor, in addition to α, in the study area at the central frequencies studied, and after comparing them with previous studies in the region, such as (Bao et al., 2011) and (Mohammad, 2012), it was found that the results in the aforementioned studies are close to these results; however, the maps, variations, and results in this research are more detailed, since it focuses on a small area within Syria compared to studies examining wide regions that may include all of Syria and its surroundings.

3- Clarifying the relationship between the change in attenuation and frequency showed a close correlation and a strong variation of attenuation values with frequency, as the quality factor increased with increasing frequency in the study area, indicating a decrease in attenuation with increasing frequency.

4- The areas of topographic elevation and the areas with high deformation in the study area have the lowest quality factor values; the first represents the Qasioun Mountain area (in the shape of a circular sector), and the second represents the area closest to the Dead Sea Fault.

This research represents an important part of the steps toward completing attenuation calculations within Syria in general and southern Syria in particular. The above can be summarized by noting that the study area is a region of high attenuation in the southwest, and to a lesser degree in the rest of the region, as shown in the maps studied. Attenuation also plays an important role, as its close dependence on frequency is evident through the attenuation variations observed at the different central frequencies read.

Funding: This Research is funded by Damascus University-Funder no (501100020595).

References:

1. Padhy, S. , Subhadra, N. & Kayal, J, R.,2011. Frequency-Dependent Attenuation of Body and Coda Waves in the Andaman Sea Basin, Bulletin of the Seismological Society of America, Vol. 101, No. 1, pp. 109–125.
2. Havskov J, Malone S, McCloug D, Crosson R (1989) Coda Q for the state of Washington. Bull Seismol Soc Am 79:1024–1038.
3. حمد، رندة سعد الدين (2012) تخامد الأمواج الزلزالية المحلية والإقليمية في سورية والمناطق المجاورة. رسالة دكتوراه، جامعة دمشق، دمشق.
4. قنواتي ،نور.(2024) النشاط السايزمي في منطقة القلمون باستخدام التسجيلات المستمرة لمحطات المركز الوطني للزلازل وشبكة جامعة دمشق .رسالة ماجستير، جامعة دمشق، دمشق.
5. Bao ,X. , Sandvol ,E. , Zor, E. , Sakin, S. , Mohamad ,R. , Gök ,R. , Mellors, R. , Godoladze ,T. , Yetirmishli ,G. , Türkelli ,N. ,(2011) , Pg attenuation tomography within the Northern Middle East . Bull . Seismol . Soc . Am . , 101 (4) : 1496-1506 . doi : https://doi.org/10.1785/0120100316 .
6. Sandvol , E. , Al – Damegh, K. , Calvert, A. , Seber, D. , Barazangi, M. , Mohamad, R. , Gök, R. , Türkelli, N. , and Gurbuz, C. (2001) . Tomographic imaging of Lg and Sn propagation in the Middle East , Pure Appl . Geophys . 158 , 1121-1163 .
7. حسين، كمال محي الدين(2012) جيولوجية سورية الإقليمية (1) (ط: 3) .دمشق: مطبعة جامعة دمشق
8. Havskov, J. Sørensen, M, B. Vales, D. Özyazıcıoğlu, M. Sánchez, G. & Li, B. (2016) Coda Q in Different Tectonic Areas, Influence of Processing Parameters. Bulletin of the Seismological Society of America, Vol. 106, No. 3. doi: 10.1785/0120150359
9. Kumar, C. H. P., Sarma, C. S. P., Shekar, M., & Chadha, R. K. (2006). Attenuation studies based on local earthquake Coda waves in the southern Indian peninsular shield
10. Havskov, J., and L. Ottemöller (1999). SEISAN earthquake analysis software, Seismol. Res. Lett. 70, 532–534.
11. Giampiccolo, E., & Tuvè, T. (2018). Regionalization and dependence of coda Q on frequency and lapse time in the seismically active Peloritani region (Northeastern sicily, italy). Journal of Seismology, 22(4), 1059–1074. https://doi.org/10.1007/s10950-018-9750-0
12. Del Pezzo E, Bianco F, Giampiccolo E, Tusa T, Tuvè T (2015) Areappraisal of seismic Q evaluated at Mt. Etna volcano.Receipt Application Risk Analysis J Seismol 19:105–119.https://doi.org/10.1007/s10950-014-9453-0
13. Parvez IA, Sutar AK , Mridula M,Mishra SK, Rai SS (2008) Coda Q estimates in the Andaman Islands using local earthquakes.Pure Appl Geophys 165:1861–1878
14. Pulli JJ (1984) Attenuation of coda waves in New England. Bull Seismol Soc Am 74:1149–1166